Hindawi
Shock and Vibration
Volume 2018, Article ID 4179312, 13 pages
https://doi.org/10.1155/2018/4179312

Research Article

Effect of Axial Vibration on Sliding Frictional Force between Shale and 45 Steel

Wu Hao[1], **Chen Ping**[1], **Liu Yang**[1,2] **and Ma Tianshou**[1]

[1]*State Key Laboratory of Oil and Gas Reservoir Geology and Exploitation, Southwest Petroleum University, Chengdu, Sichuan 610500, China*
[2]*Department of Mechanical Engineering, The University of Melbourne, Melbourne, VIC 3010, Australia*

Correspondence should be addressed to Chen Ping; chenping@swpu.edu.cn and Liu Yang; liuyang2013swpu@163.com

Received 17 October 2017; Accepted 25 December 2017; Published 24 January 2018

Academic Editor: Marc Thomas

Activating drill string vibration is an effective means to mitigate the excessive drag encountered during drilling complex-structure wells. However, the Coulomb model cannot describe the sliding friction behavior between drill string and borehole rock with imposed axial vibrations. To solve this problem, a specially designed experimental setup was utilized to investigate the characteristics of axial vibrating-sliding coupling friction. The results indicate that when vibration velocity is greater than sliding velocity, axial vibration can significantly reduce friction force between contact surfaces. Its friction reduction mechanism embodies not only the changes of instantaneous friction force, but also friction coefficient. Meanwhile, a friction coupling model was established based on the Hertz contact theory and Dahl model. The corresponding computational program was developed in Matlab/Simulink environment. The calculation results are in good agreement with the experimental results, verifying the validity of the present method. Furthermore, to overcome the shortcoming of Dahl model, a dynamic friction coefficient model was proposed to evaluate the friction-reducing effect of axial vibration using dimensional analysis method. The model parameters under different lubrication conditions were retrieved through inverse calculation with experimental data. This method provides a new solution for evaluating the friction-reducing effect of hydraulic oscillator and optimizing its placement.

1. Introduction

The frictional contact problem between drill string and borehole rock is a basic research topic in drilling engineering [1–3]. Excessive drag encountered in complex-structure wells (such as horizontal wells, extended-reach wells, and multilateral wells) with the sliding drilling mode severely restricts the improvement of rate of penetration (ROP) and ultimate extension distance [4, 5]. According to the statistics from Roberto et al. [6], approximately 30% of the total drilling time was spent to adjust wellbore trajectory and control azimuth with slide drilling mode during drilling directional or horizontal wells, and the produced excessive drag made it progressively more difficult for the drill string to slide smoothly. Definitely, the overall gross ROP is much less during sliding mode with a steerable motor than during rotating mode. It is not unusual to have the sliding ROP be as much as 70% less than the rotating ROP. Therefore, how to reduce the excessive drag caused by drilling complex-structure wells with sliding mode has become a key issue needing urgent solution in complex oil and gas development [7, 8].

However, recently, tribology research has moved toward a combination of analysis and control and has even been extended to control tribological properties. Through experimental and theoretical methods, many studies have demonstrated that the frictional force can be dramatically mitigated by imposing mechanical vibrations [9, 10]. Roper and Dellinger [11] first proposed the technical ideas of reducing frictional force during slide drilling in the form of invention patent; namely, activating axial vibrations on the drill string using vibrator can lower the frictional force between drill string and borehole rock. The technical idea expedites the development and application of several friction reduction technologies and corresponding drag-reduction tools, among which the most typical and used commercially is the hydraulic oscillator developed by National Oilwell Varco

[8, 12, 13]. Meanwhile, the research on friction reduction effect of different vibration modes has also achieved positive progress. Barakat et al. [14] simulated the effect of axial vibration on axial force transmission via experiments. The results show that axial vibration can significantly enhance the axial force transmission in the frequency range of 5 Hz to 20 Hz and reduce the frictional force in the range of 30%~100%. Newman et al. established a full-sized test rig for modeling the influence of vibration on drag reduction and demonstrated that axial vibration is more effective in decreasing frictional force than lateral and torsional vibration. According to Hamilton's principle and finite element method, a full-hole drill-string dynamics model for horizontal well was established by Gee et al. [2]. The simulation results show that the friction reduction effect of transverse vibration is merely 30%~70% of that of axial vibration. These results provide the basis support for the structural design and optimization of vibration drag-reduction tools, but all is insufficient to quantitatively evaluate the friction reduction effect of axial vibration. The reason lies in that the abovementioned theoretical and experimental studies were carried out by using Coulomb friction model.

Tribological research suggests that friction model can be divided into static model and dynamic model, which depends on whether the tribological phenomena are described by using differential equations or not. The classical Coulomb model falls into the category of the static model. However, the dynamic friction model can describe not only the static characteristics but the dynamic ones of frictions. The pioneering research on dynamic friction model for different materials was conducted by Dahl [15] and therefore the Dahl model became one of the earliest dynamic friction models. Thereafter, dynamic models, such as Dupont model [16, 17], LuGre model [18], Leuven model [19], and GMS model [20], were derived from the Dahl model. These models used the Dahl model's properties to describe preparatory displacement-slip friction and to predict friction hysteresis. However, the challenge of dynamic parameters identification has unfavorable effect on the application of these models in drilling engineering. Comparatively speaking, the Dahl model is studied and applied widely because it can be implemented with ease and few parameters need to be tuned. Meanwhile, many scholars [21–24] investigated the effect of axial vibration on steel-steel sliding friction behavior through experiment. The results reveal the friction reduction mechanism of axial vibration (i.e., "friction vector effect") and verify the validity and practicability of Dahl model. Nevertheless, these studies mainly focus on the influence of axial vibration with high frequency and low amplitude on sliding friction and do not take into account the effects of drilling fluids lubrication. Obviously, it has great difference with the actual operating situation of hydraulic oscillator. Wang et al. [25] studied the effect of axial vibration and transverse vibration on steel-rock plane sliding friction pairs, however, with a wide distribution of vibration frequencies and without consideration of the drilling fluids' lubrication effect.

Thus, in order to evaluate the friction reduction effect of axial vibration quantitatively, a specially designed laboratory test rig was used to simulate the vibration friction between shale and steel in downhole environment. A friction coupling model has been established based on the Hertz contact theory and the Dahl model. The calculation results using the present model are in good agreement with the experimental results, verifying the validity of the present model and method. Furthermore, considering the limitations of the Dahl model, a dynamic friction coefficient model is proposed by using dimensional analysis method, which can quantitatively evaluate the friction reduction effect of axial vibration. The model parameters are retrieved through inverse calculation with experimental data and the expressions formula of dynamic friction coefficients under different lubrication conditions was obtained. This method provides a new solution for evaluating the friction reduction effect of hydraulic oscillator and optimizing its placement.

2. Experiment

2.1. Sample Preparation. The 45 steel was selected as the metal specimen and was processed into a cuboid steel plate with the dimension of 170 mm × 30 mm × 5 mm. The shale samples, a cubic core (40 mm × 40 mm × 40 mm) with a face of the rock polished into an arc shape (arc radius was 25 mm), were cut along the bedding direction from Wufeng formation in Changning area, Sichuan Basin. After processing, abrasive paper and a stone grinding machine were used to polish the steel plate surface and shale sample surface, respectively. To eliminate size error and ensure measured data quality, the accuracy requirement was that the thickness error of metal specimen shall be no greater than 0.5 mm and the radius error of curvature of shale sample cannot exceed 0.3 mm. Here the accuracy requirement was defined by us; experimenters can adjust it appropriately according to the actual situation. The MFT-4000 multifunctional material performance tester was used to measure the surface roughness of metal specimen and shale sample (0.413 μm and 1.287 μm, resp.). In addition, considering the effect of drilling fluid lubricity on tribological properties, three typical drilling fluid systems were adopted as the lubricant medium. Their performance parameters were shown in Table 1.

2.2. Experimental Method. Figure 1 shows the experimental setup that was used to investigate the vibration friction behavior between the rock and steel friction pair in different lubricating environment. It was composed of four parts, including the axial vibration system, the axial sliding system, the normal force loading system, and the load measurement system and control units. The main technical parameters are shown in Table 2. During the experiment, the shale sample was fixed on the pillar by using a bolt (Figure 1). The pillar was connected with electrodynamic vibration shaker, which provided the impetus source for axial vibration and could control amplitude and frequency. The metal specimen slides with a constant velocity along vertical direction under the driving of line-glide rail, and the slide velocity was adjusted by electric cabinet. The shale sample touched the steel specimen surface closely. The normal force was imposed on the steel specimen through four universal balls. The magnitude of the

Table 1: Drilling fluid performance parameters.

Parameters	ρ (g/cm^3)	FV (s)	YP (Pa)	PV (mPa·s)	GS (Pa)	OWR	Lubricant
WBM	1.75	45~75	5~14	14~38	2~6/4~14	/	Alcohol substance
OBM	2.1	45~100	5~20	24~75	2~8/3~15	80~90/20~10	White oil
SBM	1.95	50~100	6~18	40~85	3~6/4~15	/	Ester

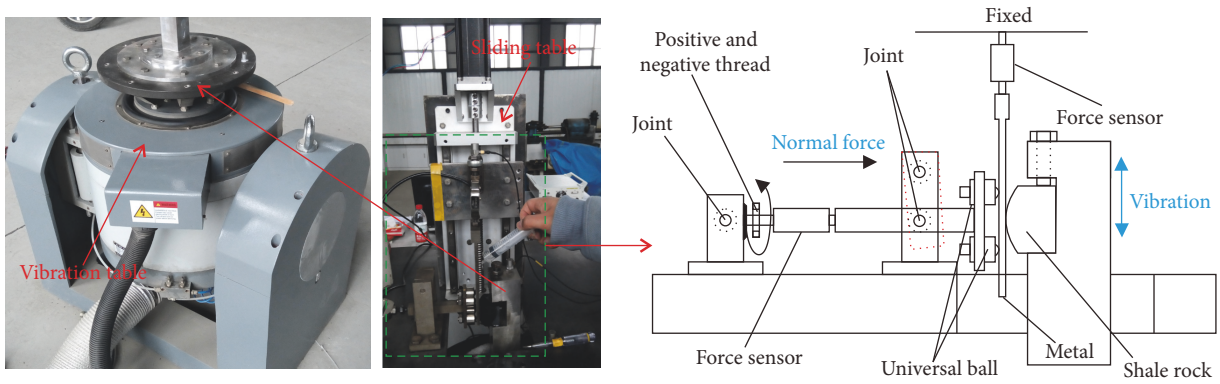

Figure 1: Test rig for axial vibrating-sliding friction coupling.

Table 2: Main technical parameters of test rig.

Parameters	Value	Unit
Vibration frequency	5~3000	Hz
Vibration amplitude	1~50	mm
Vibration acceleration	<100	m/s^2
Sliding velocity	<5	mm/s
Effective sliding distance	<200	mm
Normal force	<200	N

normal force was controlled by specially processed positive and negative thread. The load cell was utilized to measure the driving force and normal force. In addition, experimental parameters, such as vibration acceleration and sliding displacement, were collected and processed in real time.

The shale rock was cut into a rectangular shape with a face of the rock polished into an arc shape to maintain good contact with the steel specimen. However, due to the stiffness difference of rock sample and steel specimen, the cambered surface will quickly wear down to a narrow plane, and the wear loss on the curved surface was closely related to normal force, lubricant medium, and so on. Thus, the contact mode of the two objects was no longer line/plane contact, but plane/plane contact. Actually, the lab tests found that the wear rate was initially very quick and then tended to reduce and stabilize. Hence, to eliminate the influence of contact mode changes in the experiments, the shale sample was allowed to wear in the experimental setup for about 5 min as a pretest. After the wear area becomes close to stable as the contact area increases, set testing conditions and carry out related experiment according to the experimental scheme. Before the fluid lubrication experiment, the shale sample was firstly soaked in corresponding drilling fluid for approximately 30 min, taken out, and fixed on the rock sample clamping system. The syringe was used to aspirate drilling fluid, which was then slowly injected on the contact surface to stimulate the actual drilling.

2.3. Experimental Scheme

2.3.1. Experimental Scheme for Sliding Friction. The determination of friction coefficients between drill string and borehole rock serves as not only the basis for study on dynamic friction theory, but the key factor for prediction of friction force in horizontal well. In general, sliding friction between contact surfaces brings about various degrees of heating, deformation, and frictional wear with changes of sliding velocity, normal force, or lubricant medium. These factors have certain influence on friction coefficient test result. But generally speaking, the influence degree is quite limited. Therefore, this section just measures the friction coefficient under different lubricant conditions, including dry, water, water-based mud (WBM), synthetic-based mud (SBM), and oil-based mud (OBM), and neglects the effect of the abovementioned factors.

In this experimental scheme, the normal force was determined by using Hertz contact theory and the equivalence principle of contact stress. Due to the rapid wear of shale surface, the contact mode between the shale sample and metal specimen was no longer a line/plane contact; it was, instead, a plane/plane contact, as shown in Figure 2. The contact stress between hydraulic oscillator and borehole rock can be calculated by the following equations [26]:

$$q_c = 9.81\pi\left(r_{co}^2 - r_{ci}^2\right)\left(\rho_s - \rho_m\right) \quad (1)$$

$$\sigma_d = \frac{\sqrt{q_c\left(1/r_w - 1/r_{co}\right)}}{\sqrt{\pi\left(\left(1-\mu_r^2\right)/E_r + \left(1-\mu_s^2\right)/E_s\right)}}, \quad (2)$$

where q_c is the HOT weight per unit length in the mud, N/m; r_{co} is the outer diameter of HOT, m; r_{ci} is the inner diameter

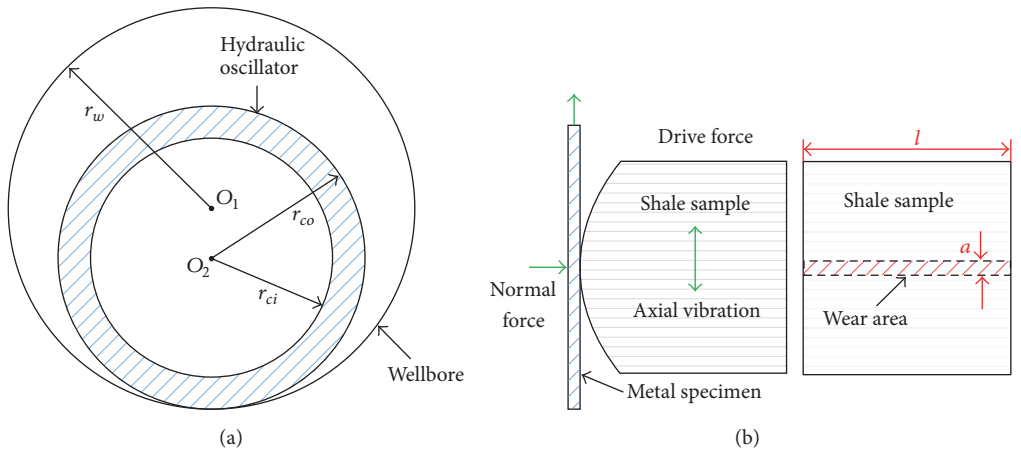

FIGURE 2: Contact mode simplification model: (a) contact mode between hydraulic oscillator and wellbore rock; (b) contact mode between shale sample and metal specimen.

of HOT, m; ρ_s is the density of steel, kg/m^3; ρ_m is the density of mud, kg/m^3; r_w is the inner diameter of wellbore, m; σ_d is the contact stress between the AOT and wellbore, MPa; E_r is the elasticity modulus of shale rock, GPa; E_s is the elasticity modulus of steel, GPa; and μ_s and μ_r are Poisson's ratio of steel and shale rock, respectively.

Figure 2(b) shows the contact mode between shale rock and metal specimen. The contact stress between the two objects can be presented as

$$\sigma_e = \frac{F_e}{al}, \tag{3}$$

where F_e is the normal force acting on the steel specimen, N; a is the width of the rock wear area, m; and l is the width of the steel specimen, m.

According to the equivalence principle of contact stress, simultaneous equations (2) and (3), the normal force under experimental conditions can be obtained:

$$F_e = \frac{al\sqrt{q_c\left(1/r_{co} - 1/r_w\right)}}{\sqrt{\pi\left(\left(1-\mu_r^2\right)/E_r + \left(1-\mu_s^2\right)/E_s\right)}}. \tag{4}$$

According to the actual borehole size and the design parameters of hydraulic oscillator [5], the determined normal force for sliding friction experiment is about 150 N.

2.3.2. Experimental Scheme for Axial Vibrating-Sliding Friction Coupling. Vibration intensity is generally described by amplitude u and frequency f, which directly influence the friction reduction effect of axial vibration. Besides, sliding velocity v_d, normal force F_N, and lubrication medium have different effects on friction force in this case. Therefore, in order to analyze the influence of these factors on friction reduction effect of axial vibration, the orthogonal experiment method was employed in designing this part of experimental scheme. The factors and levels graphs are listed in Table 3, among which vibration parameters refer to the operating parameters of hydraulic oscillator. The sliding velocity refers to the corresponding ROP in actual drilling conditions (assuming the average ROP during sliding drilling is 7 m/h). The determined normal force for this experiment is about 150 N.

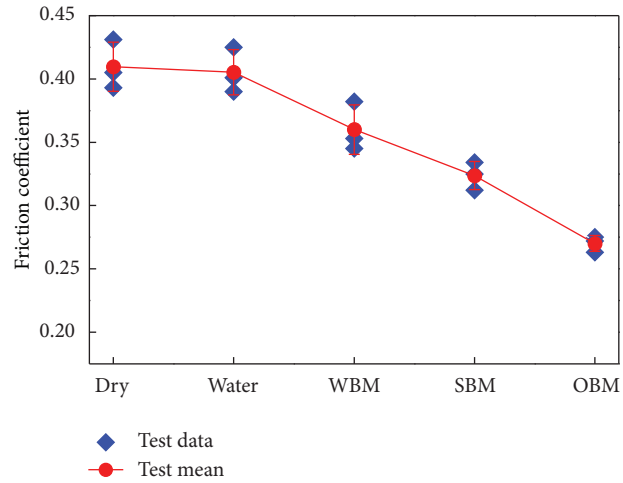

FIGURE 3: Corresponding sliding friction coefficients of different lubricant media.

2.4. Experimental Results

2.4.1. Results of Sliding Friction Coefficient Experiment without Vibration. Through the processing of the real-time sampling data (including driving force and normal force), the friction coefficient testing results for different lubricant media can be obtained, as shown in Figure 3. In comparison with the experimental results of dry friction, the measured friction coefficients for WBM, SBM, and OBM are 0.36, 0.32, and 0.27, respectively, and decrease by 12.2%, 21.9%, and 34.1%, respectively. This indicates that the lubricant applied on the contact surfaces can reduce friction coefficient to some degree and the lubrication effect varies significantly with the lubricant media. The friction reduction effect of different

Table 3: Factor level in orthogonal experiment.

Factors	Lubricant	u (mm)	f (Hz)	v_d (mm/min)	F_N (N)
(1)	Dry	3	15	20	30
(2)	Water	4	16	40	60
(3)	WBM	5	17	60	90
(4)	OBM	6	18	90	120
(5)	SBM	8	20	120	150

Table 4: Summary of experimental results.

Number	Lubricant	u (mm)	f (Hz)	v_d (mm/min)	F_N (N)	Null	F_{sf}	F_{df} (N)	u_{df}
VS1	Dry	3	15	20	30	1	12.29	2.82	0.094
VS2	Dry	4	16	40	60	2	24.58	5.88	0.098
VS3	Dry	5	17	60	90	3	36.87	9.27	0.103
VS4	Dry	6	18	90	120	4	49.16	14.4	0.12
VS5	Dry	8	20	120	150	5	61.45	16.8	0.112
VS6	Water	3	16	60	150	5	60.80	18.45	0.123
VS7	Water	4	17	90	30	1	12.16	3.42	0.114
VS8	Water	5	18	120	60	2	24.32	6.36	0.106
VS9	Water	6	20	20	90	3	36.48	8.55	0.095
VS10	water	8	15	40	120	4	48.64	11.64	0.097
VS11	WBM	3	17	120	60	4	21.60	5.34	0.089
VS12	WBM	4	18	20	90	5	32.40	5.49	0.061
VS13	WBM	5	20	40	120	1	43.20	8.4	0.07
VS14	WBM	6	15	60	150	2	54.00	11.25	0.075
VS15	WBM	8	16	90	30	3	10.80	2.34	0.078
VS16	OBM	3	18	40	150	3	40.50	5.4	0.036
VS17	OBM	4	20	60	30	4	8.10	1.02	0.034
VS18	OBM	5	15	90	60	5	16.20	2.58	0.043
VS19	OBM	6	16	120	90	1	24.30	4.05	0.045
VS20	OBM	8	17	20	120	2	32.40	3.36	0.028
VS21	SBM	3	20	90	90	2	29.13	6.39	0.071
VS22	SBM	4	15	120	120	3	38.84	9.36	0.078
VS23	SBM	5	16	20	150	4	48.55	9.3	0.062
VS24	SBM	6	17	40	30	5	9.71	1.95	0.065
VS25	SBM	8	18	60	60	1	19.42	4.02	0.067

lubricant media from high to low is OBM > SBM > WBM > water > dry.

2.4.2. Results of Axial Vibrating-Sliding Friction Coupling Simulation Experiment. Table 4 shows the friction force testing results under different experimental conditions, among which F_{sf} denotes the sliding friction without regard to the effect of vibration; F_{df} denotes the average sliding friction force in an vibration cycle; and u_{df} denotes average dynamic friction coefficient, $u_{df} = F_{df}/F_N$. It is not difficult to see that axial vibration can significantly reduce the sliding friction force on the contact surface. Due to the influence of electrical signals, vibration signals, and ambient noises during the experiment, the measured data are generally complex and are of multitone signals. Therefore, the Empirical Mode Decomposition (EMD) [27] has been adopted in this paper to decompose the experimental data into number of Intrinsic Mode Functions (IMFs). The decomposition of the measured data $x(t)$ is as follows [28]: ① Sample the time domain signal $x(t)$. ② Identify all maxima and minima for the sampled data points $x(n)$. ③ Generate its upper and lower envelop, $e_{\min}(n)$ and $e_{\max}(n)$, and use cubic spline interpolation. ④ Calculate the mean $m(n)$ for the upper and lower envelop, $m(n) = (e_{\min}(n) + e_{\max}(n))/2$. ⑤ Extract the mean from time series and define difference of $x(n)$ and $m(n)$ as $h(n)$, $h(n) = x(n) - m(n)$. ⑥ Check the properties of $h(n)$, that is, SD $= \sum((\text{prev}(h) - h)^2/\text{prev}(h)^2)$. If SD < 0.3, repeat steps ①~⑤ until the residual satisfies some stopping criterion. ⑦ Then the signal $x(n)$ can be expressed as $x(n) = \sum_{i=1}^{n} c_i(n) + r_n(n)$. Once the IMFs are obtained, Fast Fourier Transform (FFT) is applied to the IMFs to get the frequency domain of the original decomposed signals. It should be noted that fluid

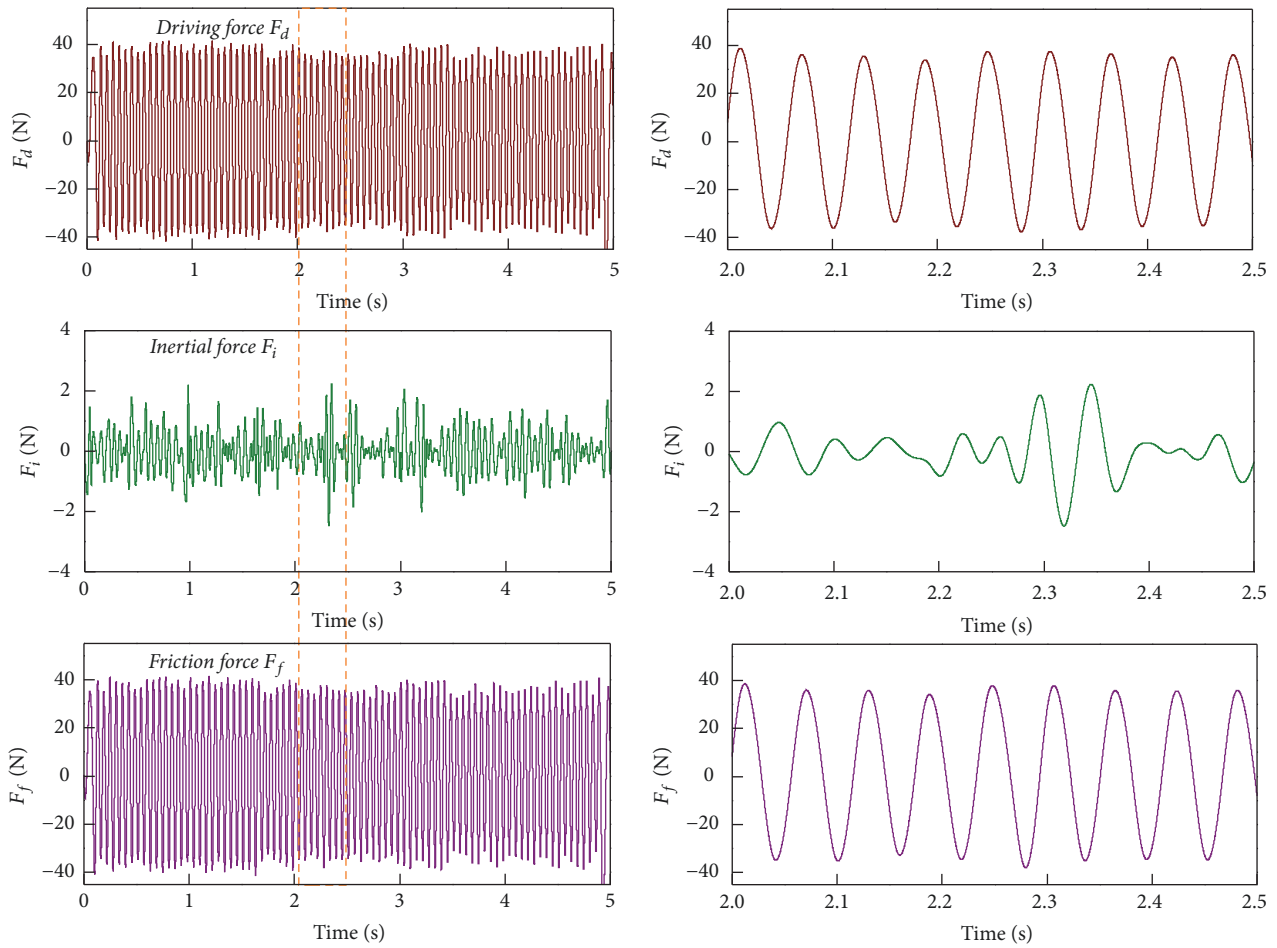

FIGURE 4: Experimentally determined characteristics of forces F_d, F_i, and F_f during vibrating-sliding friction coupling. Experiment parameters: dry, $u = 5$ mm, $f = 17$ Hz, $v_d = 60$ mm/s, and $F_N = 90$ N.

lubrication does not alter the changing pattern of friction curves in the process of experiment. Thus, here only tick off the friction force measured data under dry and OBM conditions as follows, as shown in Figures 4 and 5.

During the investigations, the sensor force was utilized to measure the driving force of metal specimen and changes in acceleration of the metal specimen were also measured in the direction of the sliding motion. Consequently, it was possible to determine the profile of the inertia force F_i ($F_i = -m \cdot a_m$) sliding specimen. Knowing the characteristic of the driving force and inertia force of sliding specimen, Newton's second law can be utilized to determine the time-related variability of friction forces acting on the contact surface between shale sample and metal specimen. The experimentally determined time characteristics of F_f, F_i, and F_d under dry and OBM conditions were illustrated in Figures 4 and 5. According to the experiment results, the following conclusions can be made: (1) the measured sliding friction force shows a periodical change in the experimental stage; thus it can be stated that the total friction force decreases significantly over one vibration cycle when compared with nonvibration conditions; (2) when the vibration velocity amplitudes are greater than the sliding velocity, the value and direction of the instantaneous friction force are changed, which is the root cause of vibrating friction reduction; (3) the axial sliding of metal specimen is inevitably affected by vibration transmission from shale sample, which causes the inertia force of metal specimen. Besides, the inertia force of metal specimen is associated with normal force and lubrication medium; (4) according to the experiment data distribution rule, the measured driving force (F_d) and inertia force (F_i) with OBM lubrication are more stable than other conditions, which indicates that fluid lubrication can mitigate the vibration transmission to some degree.

3. Axial Vibrating-Sliding Friction Coupling Model

3.1. Basic Assumptions. To facilitate the establishment of the axial vibrating-sliding friction coupling model between metal specimen and shale sample, the following assumptions are made:

(1) The surfaces of shale sample and metal specimen are relatively smooth and the essence of interactions between these two objects within the contact zone is presented as contact deformation between asperities.

(2) Neglect the system damping; namely, $h_d = 0$.

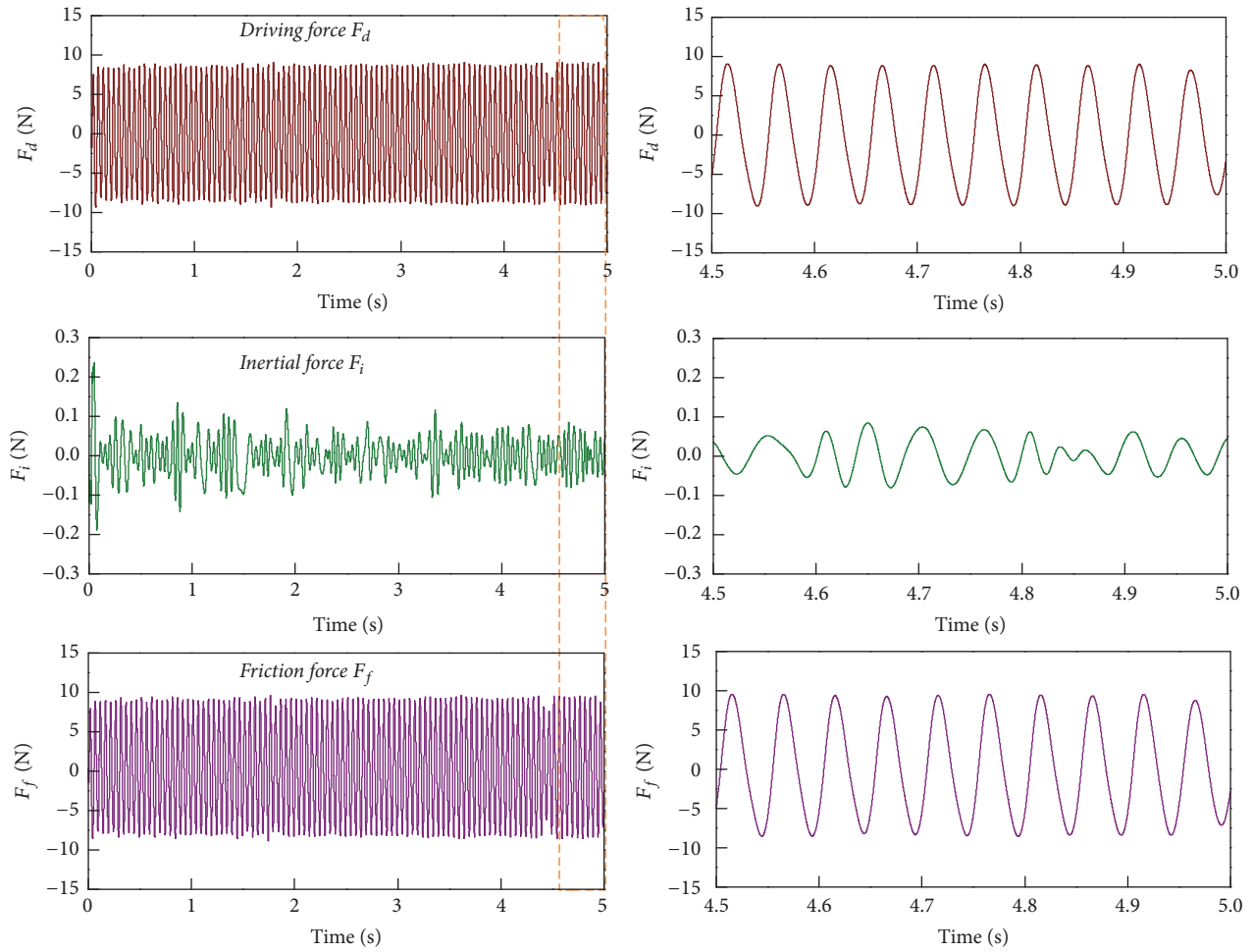

FIGURE 5: Experimentally determined characteristics of forces F_d, F_i, and F_f during vibrating-sliding friction coupling. Experiment parameters: OBM, $u = 4$ mm, $f = 20$ Hz, $v_d = 60$ mm/s, and $F_N = 30$ N.

(3) The contact between rock sample and steel specimen follows the Hertz theory.

(4) The metal specimen slides with a constant velocity along the vertical direction under the driving of line-glide rail.

(5) The vibrating motion of the shale rock remains harmonic and takes the form $u = u_0 \sin(\omega t)$, and the amplitude of vibration velocity is defined as $v_a = u_0\omega$.

3.2. Model Description. Based on the above assumption, the friction behaviors between metal specimen and shale sample can be simplified into the interaction model, as shown in Figure 6(a). The distribution of the forces acting on the metal specimen is given in Figure 6(b).

The vector equation for the metal specimen moving on a vibration plane in a stationary reference system can be expressed as

$$m\vec{a} = \vec{F_d} + \vec{F_g} + \vec{F_e} + \vec{F_F} + \vec{F_N}, \tag{5}$$

where m denotes the mass of the body, kg; $\vec{a}$ denotes acceleration, m/s^2; $\vec{F_d}$ is the driving force, N; $\vec{F_g}$ is the force of gravity, N; $\vec{F_e}$ is the external load perpendicular to the sliding surface, N; $\vec{F_F}$ is the friction force, N; and $\vec{F_N}$ is the support's normal reaction, N.

Correspondingly, if the metal specimen slides along the vertical direction, (5) can be simplified into

$$m\frac{d^2x}{dt^2} = F_d - F_F - F_g. \tag{6}$$

Because the metal specimen is inevitably affected by the vibration transmission from the shale sample during sliding, the driving force of the whole system is a variable depending on relative displacements of point A and point B:

$$F_d = k_d\zeta = k_d\left(v_d t - x\right). \tag{7}$$

In the Coulomb friction model, it is assumed that the interacting contact surfaces are perfectly rigid. The friction force considering sliding and axial vibration can be written as

$$F_F = \mu F_N \operatorname{sgn}\left(v_r\right). \tag{8}$$

In the Dahl model, it is assumed that the magnitude of the friction force is correlated with the elastic deformation

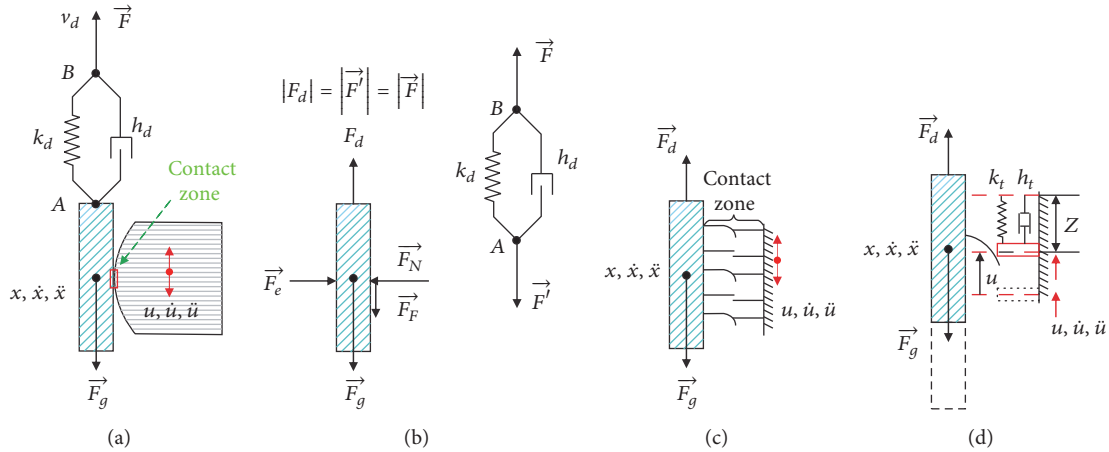

FIGURE 6: Simplified model for the analysis of friction in the presence of axial sliding and vibration. (a) Interaction model of the sliding-vibration system; (b) distribution of forces acting on the sliding body; (c) distribution of asperities in the contact zone; (d) elastic deformation of the contact zone in the presence of axial vibration.

of the contact zone (Figures 6(c)-6(d)). The mathematical description of the Dahl model can be expressed as follows:

$$\frac{dz}{dt} = v_r \left[1 - \frac{k_t}{\mu F_N} \operatorname{sgn}(v_r)\, z\right]^{\alpha}$$
$$F_F = k_t z, \tag{9}$$

where z denotes the elastic strain of the contact in the tangential direction, mm; k_t denotes the tangential contact stiffness coefficient, N/mm; and v_r is the relative velocity of sliding body (metal specimen) in relation to vibrating object (shale sample), mm/s.

3.3. Model Solution and Verification. According to (9), it can be found that the friction force calculated by the Dahl model is correlated with tangential contact stiffness coefficient and the elastic deformation of the asperities in the contact zone. And its integral expression is a piecewise function controlled by the relative velocity of the sliding body in relation to the vibration plane, which is bad for the model solution. Thus, based on the calculation model shown in (5)–(9), a computational program is developed in the Matlab/Simulink environment [4, 29]. The Coulomb and Dahl models were adopted to calculate the changes of friction force with the time and to compare the results with the experimental data. The comparison results were shown in Figure 7. It can be clearly noticed that the numerical results obtained by Dahl model agree well with experiment data no matter what lubrication medium is adopted. This illustrates that the Dahl model has certain advantages to describe the friction coupling characteristics of sliding with an imposed axial vibration.

4. Analysis and Discussion

4.1. Comparison of Experimental Setup. Activating mechanical vibration is an effective means of mitigating the system friction effect. Thus, domestic and foreign scholars have established different experimental setups to simulate the friction reduction effect of various vibration modes, among which the two most representative test units are shown in Figure 8. Compared with the present experimental setup, the differences lie in the following.

(1) Normal Force Loading System. The test units built by Leus and Gutowski [23] and Wang et al. [25] have a common point that the sliding specimen (upper specimen) was not constrained in the normal direction and relied only on gravity to maintain effective contact with the vibration specimen (bottom specimen). But as mentioned above, axial vibration can inevitably cause normal vibration, resulting in unstable normal force. Thus, if without normal constraint, the normal vibration induced by axial vibration may be more significant, then affecting the accuracy of experimental results. To resolve this problem, a normal force loading system is specially designed in these test units. Although there still is vibration transmission, the effect of transverse vibration becomes less.

(2) Vibration Direction. The test rig established in literatures activates axial vibration along the horizontal direction, while that established in this paper brings about axial vibration along the vertical direction by using electrodynamic vibration shaker. It makes the driving force measured in this experiment include the gravity of metal specimen, which is required to be eliminated during experimental data processing.

(3) Experimental Parameters. Leus and Gutowski [23] mainly investigated the effect of applied vibrations with high frequency (f = 3900 Hz) and low amplitude (u = 0.7 μm) on the friction force characteristics of steel-steel friction pair. However, Wang et al. [25] studied the friction pairs between steel and steel, sandstone, and shale. The operating frequencies of their experiments were varied uniformly from 0 Hz to 500 Hz with 100 Hz steps. The exciting forces on bottom specimen were 0 N, 40 N, 80 N, 120 N, 160 N, and 200 N. It is not hard to see that the vibration frequencies adopted in the literatures are significantly higher than frequency parameters

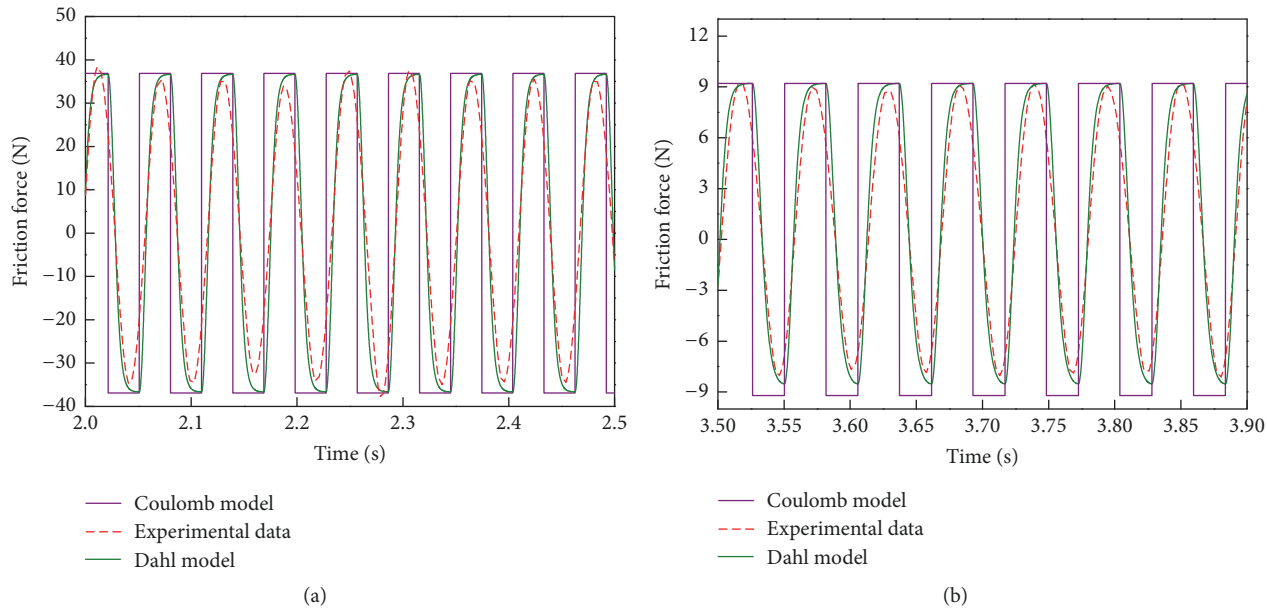

Figure 7: Comparison between the numerical simulation and experimental results: (a) dry, $u = 5$ mm, $f = 17$ Hz, $v_d = 60$ mm/s, and $F_N = 90$ N; (b) OBM, $u = 4$ mm, $f = 20$ Hz, $v_d = 60$ mm/s, and $F_N = 30$ N.

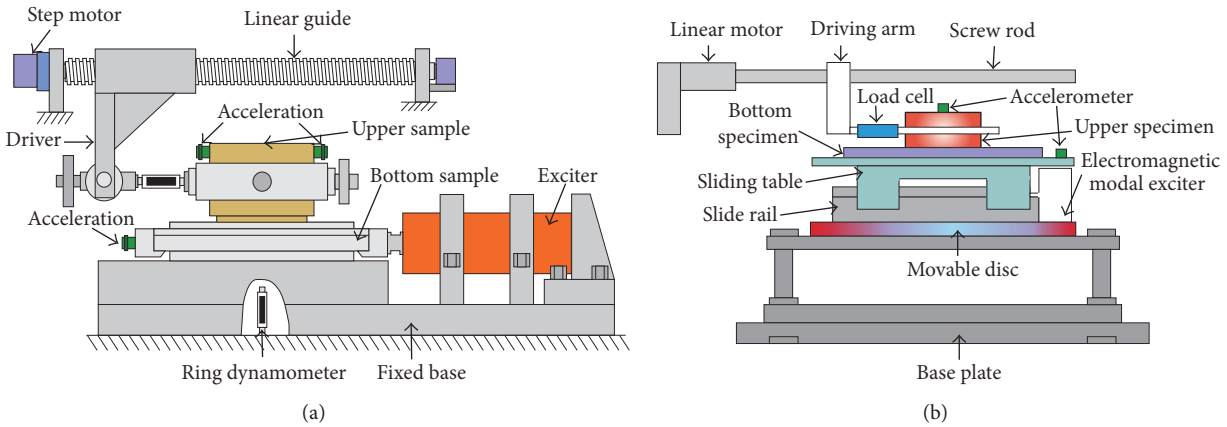

Figure 8: Sliding friction experimental setups considering vibration effect: (a) reproduced after Leus and Gutowski [23]; (b) reproduced after Wang et al. [25].

(f = 15~20 Hz) employed in this paper and the amplitude parameters are significantly less than those in this paper. Actually, due to the constraint of wellbore shape and drill string, it is impractical to activate high-frequency vibration at downhole condition.

(4) Experimental Environment. Both Leus and Gutowski [23] and Wang et al. [25] carried out friction experiments in the indoor environment. However, this experimental scheme takes into account not only ambient temperature and relative humidity, but also the effect of fluid lubrication.

4.2. The Effect of Tangential Contact Stiffness Coefficient. The friction force calculated by the Dahl model is affected by many factors, such as vibration parameters, tangential contact stiffness coefficient, asperity deformation, and the properties of contact material. Thus, rapid identification and obtaining these parameters have direct impact on the accuracy of calculated friction force. And the tangential contact stiffness coefficient is one of the most complicated parameters that need to be determined. Generally, when the tangential force imposed on the sliding object is gradually unloaded to its initial value, the sliding object can hardly return to its original position, but some certain residual displacement (w) remains. The tangential force-displacement curve will also show an elliptic envelope during the unloading-reloading cycles, the gradient of which is the tangential contact stiffness coefficient, as shown in Figure 9. However, the function relation between tangential stiffness force and displacement during loading and unloading remains unclear. This leads to difficulties in obtaining tangential contact stiffness coefficient. Therefore, fuzzy mathematical methods, such as genetic

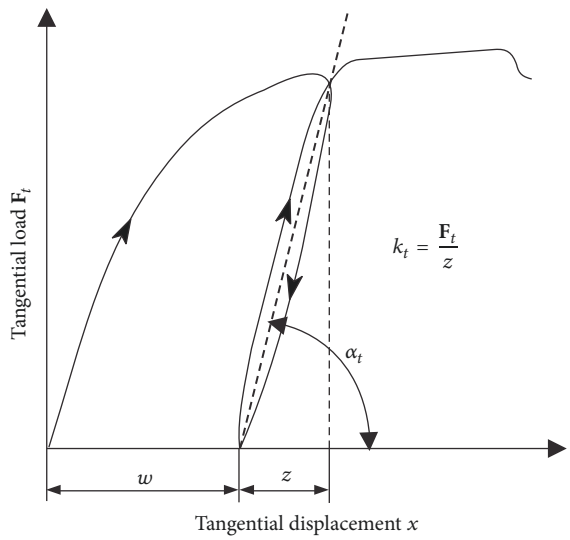

FIGURE 9: Elastic predisplacement between contact surfaces [24].

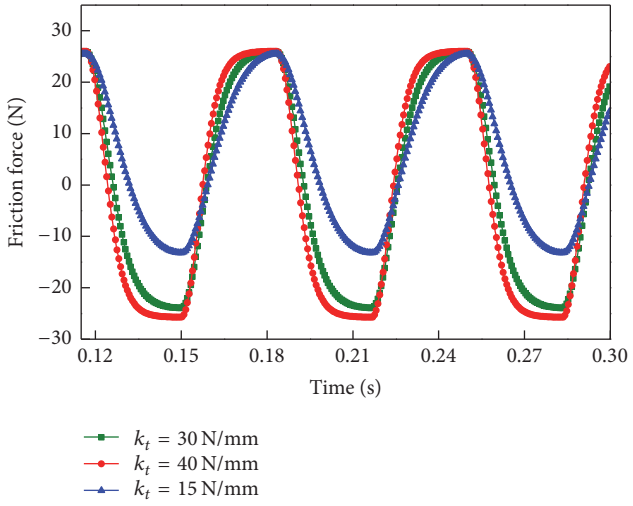

FIGURE 10: Influence of tangential contact stiffness coefficient on the change in friction.

algorithm, improved genetic algorithm, and particle swarm algorithm, are commonly utilized for the identification of model dynamic parameters.

Figure 10 shows the influence of tangential contact stiffness coefficient on the reduction in friction caused by axial vibrations for a constant sliding velocity (v_d = 0.001 m/s) and vibrating velocity (v_a = 0.534 m/s). It can be clearly noticed that the friction force calculated with Dahl model is very sensitive to tangential contact stiffness coefficient. The instantaneous friction force decreases with increasing tangential contact stiffness coefficient. By comparison of the changing features of the friction force between k_t = 30 N/mm and k_t = 40 N/mm, we find that the influence of the vibration amplitude on the reduction in friction decreases gradually. Thus, to facilitate the application of Dahl model in drilling engineering, it is necessary to overcome the difficulties in identifying dynamic parameters by means of theoretical analysis and experimental simulation.

4.3. Limitations of Dynamic Friction Models. Through theoretical computation and experimental comparison, it can be found that Dahl model can accurately describe the behavior of sliding friction with an imposed axial vibration to some extent. Consequently, Dahl model can provide theory foundation for analyzing friction reduction effect of hydraulic oscillator and optimizing its placement [29]. However, since the integral expression of Dahl model is a piecewise function, there are some difficulties in solving the governing problems. More importantly, the solution precision and computational divergence are closely related to the calculation time step and length of elements [5]. Even if the calculation time step and length of elements are reasonable, it still requires a large amount of computation time for solving the model. Obviously, it can be a challenge for engineers to rapidly evaluate the drag-reduction effect of hydraulic oscillator by applying Dahl model. Therefore, this paper tries to establish the function of dynamic friction coefficient and vibration parameters based on dimensional analysis and experimental data, to solve the problem of friction reduction effect evaluation of hydraulic oscillator.

Through analysis it can be seen that the influence of axial vibration on friction force is affected by many factors, such as normal force, sliding velocity, vibration amplitude, and frequency. Therefore, the sliding frictional force is a function of the abovementioned factors and can be expressed as

$$F_{df} = F\left(F_N, v_d, u_0, f\right), \tag{10}$$

where F_{df} is friction force in the sliding direction (MLT^{-2}); F_N is normal force (MLT^{-2}); v_d is sliding velocity (LT^{-1}); u_0 is vibration amplitude (L); and f is vibration frequency (T^{-1}).

We assume that the sliding frictional force affected by the abovementioned factors satisfies the following functional relationship:

$$F_{df} = \eta\left[{F_N}^a \cdot {v_d}^b \cdot {u_0}^c \cdot f^d\right], \tag{11}$$

where η, a, b, c, and d are dimensionless parameters.

Substituting the dimensions of each physical quantity into (11), (11) can be expressed as

$$\left[\mathrm{MLT}^{-2}\right] = \eta\left[\left(\mathrm{MLT}^{-2}\right)^a \cdot \left(\mathrm{LT}^{-1}\right)^b \cdot (L)^c \cdot \left(T^{-1}\right)^d\right]. \tag{12}$$

After simplification, the relations of each constant coefficient can be obtained:

$$\begin{aligned} a &= 1 \\ -b &= c = d. \end{aligned} \tag{13}$$

Therefore, (11) can be simplified as

$$F_{df} = \eta F_N\left[{v_d}^{-1} \cdot u_0 \cdot f\right]^c. \tag{14}$$

Neglect the transverse vibration caused by axial vibration; that is, it is assumed that the normal force acting on the metal

Table 5: The expressions of dynamic friction coefficient under different lubrication conditions.

Medium	Fitting formula	Dynamic friction coefficient
Dry	$y = -0.36513x + 0.0284\ (R^2 = 0.73)$	$u_{df} = 1.0676\left(\frac{v_a}{v_d}\right)^{-0.36513}$
Water	$y = -0.09531x - 0.70976\ (R^2 = 0.63)$	$u_{df} = 0.1951\left(\frac{v_a}{v_d}\right)^{-0.09531}$
WBM	$y = -0.16533x - 0.6745\ (R^2 = 0.88)$	$u_{df} = 0.2116\left(\frac{v_a}{v_d}\right)^{-0.16533}$
OBM	$y = -0.20306x - 0.87549\ (R^2 = 0.82)$	$u_{df} = 0.1332\left(\frac{v_a}{v_d}\right)^{-0.20306}$
SBM	$y = -0.09244x - 0.91003\ (R^2 = 0.87)$	$u_{df} = 0.1231\left(\frac{v_a}{v_d}\right)^{-0.09244}$

specimen will remain stable in the process of axial vibration. Thus, the dynamic friction coefficient during the process of axial vibration and sliding coupling friction can be expressed as

$$\mu_{df} = \eta\left[\frac{u_0 \cdot f}{v_d}\right]^c. \tag{15}$$

Because the vibrating motion of the shale rock remains harmonic and takes the form $u = u_0 \sin(\omega t)$, the amplitude of vibration velocity can be expressed as

$$v_a = u_0\omega = 2\pi f u_0. \tag{16}$$

Substituting (16) into (15), the dynamic friction coefficient can be obtained:

$$\mu_{df} = \eta\left[\frac{u_0 \cdot 2\pi f}{2\pi v_d}\right]^c = \frac{\eta}{(2\pi)^c}\left[\frac{v_a}{v_d}\right]^c. \tag{17}$$

According to (17), it can be seen that dynamic friction coefficient has an exponential relationship with velocity ratio v_a/v_d. Figure 11 shows the plot of dynamic friction coefficient u_{df} versus v_a/v_d in logarithmic coordinates. It can be observed that u_{df} keeps a linear relationship with v_a/v_d and has a digression tendency with the increasing of v_a/v_d. Based on the linear fitting results, the parameters in (17) can be inversed. The expressions of dynamic friction coefficient under different lubrication conditions are listed in Table 5. Obviously, as long as you know the vibration parameters, the friction reduction effect of hydraulic oscillator can be rapidly evaluated by substituting the inverse dynamic friction coefficient into the traditional drag/torque model. It should be noted that the accuracy of prediction can be improved by increasing the volume of experimental data.

4.4. Influence of Normal Force. The precondition of the abovementioned dimensional analysis method is that axial vibration does not result in any other additional vibration. In other words, the normal force acting on the metal specimen will consistently remain stable during axial vibration and sliding coupling friction. Because the metal specimen is inevitably affected by the vibration transmission from the

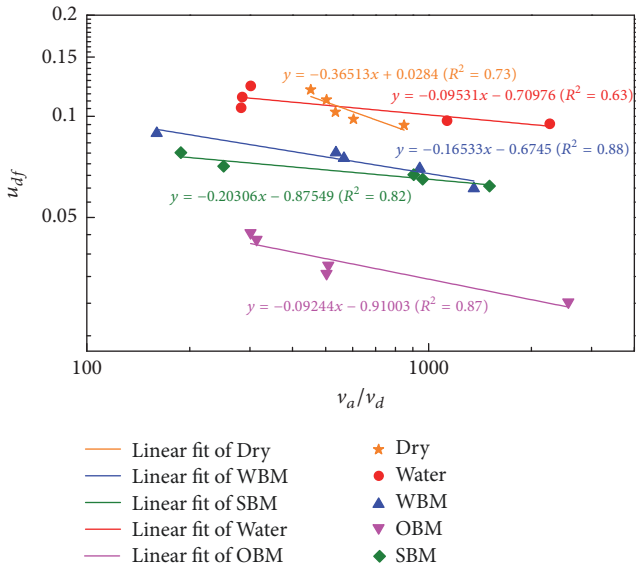

Figure 11: The plot of u_{df} versus v_a/v_d in logarithmic coordinates under different lubrication conditions.

shale sample during sliding, the assumption has a certain limitation. The monitoring data during the experiment also proves the existence of this phenomenon, as shown in Figure 12. It can be observed that the normal force follows sine function law, but the fluctuation amplitude is comparatively small. This suggests that the friction reduction mechanism of axial vibration embodies not only "friction vector effect," but also the changes of friction coefficient (which is generated by the transverse vibration induced by axial vibration). So, is it reasonable to assume a constant normal force? Since the dimensional analysis method presented in this article makes the friction reduction effect of axial vibration be regarded as dynamic friction coefficient, the influence of normal force has been attributed to the equivalent dynamic friction coefficient. Therefore, it is difficult to characterize the friction reduction mechanism of axial vibration only using dynamic friction coefficient, but it can reflect the friction reduction effect of axial vibration quantitatively. Consequently, the assumption of constant normal force is acceptable.

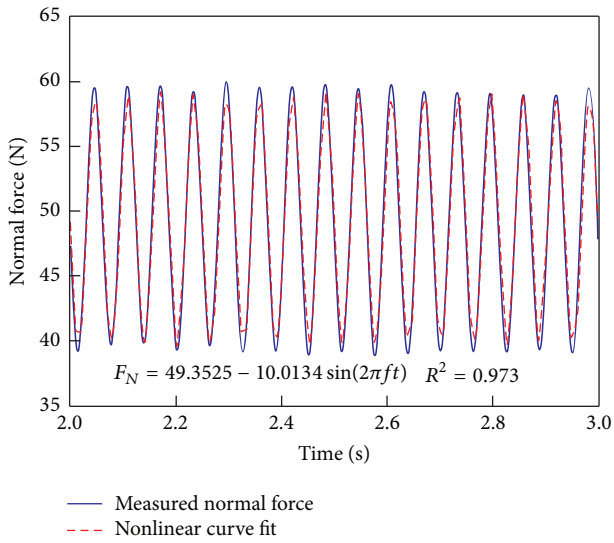

Figure 12: Normal force data obtained in real-time monitoring and the fitting curve thereof.

5. Conclusions

(1) To study the influence of axial vibration on the sliding friction behavior between the metal-shale contact surfaces, a new friction test rig is designed and used to perform the simple sliding friction experiment and axial vibrating-sliding friction coupling experiment. The friction coefficients between sliding contact surfaces under different lubrication conditions, as well as the typical characteristic curve of sliding friction under the action of axial vibration changing with time, are obtained. The experimental study shows that this test rig can basically meet the requirements on testing devices in the study of the friction reduction mechanism of axial vibration.

(2) Based on Hertz contact theory and Dahl model, the friction coupling analysis model matching with the experimental process is established and computational programs are developed in the combined Matlab/Simulink environment. According to the calculated results, compared with traditional Coulomb model, calculation results of the present model are in better agreement with the experimental results, verifying the accuracy of the present model and methods. Theoretical analysis and experimental research show that when the amplitude of vibration velocity is greater than that of the sliding velocity, the axial vibration friction reduction mechanism not only is expressed as the friction vector effect, but also is related to the changes in friction coefficients on the contact surfaces.

(3) Taking account of the limitations of the Dahl model, a dynamic friction coefficient model is proposed by using dimensional analysis method, which can quantitatively evaluate the friction reduction effect of axial vibration. The model parameters are retrieved through inverse calculation with experimental data and the expressions formula of dynamic friction coefficients under different lubrication conditions was obtained. This method provides a new solution for evaluating the friction reduction effect of hydraulic oscillator and optimizing its placement.

Conflicts of Interest

The authors declare no conflicts of interest.

Acknowledgments

This work was supported by the National Science and Technology Major Project of China (Grant no. 2016ZX05022-01), the Young Elite Scientists Sponsorship Program by CAST (Grant no. 2017QNRC001), and the National Natural Science Foundation of China (Grant no. 51604230).

References

[1] K. R. Newman, T. G. Burnett, J. C. Pursell, and O. Gouasmia, "Modeling the affect of a downhole vibrator," in *Proceedings of the The SPE/ICoTA Coiled Tubing Well Intervention Conference and Exhibition. Society of Petroleum Engineers, 31 March-1*, Woodlands, Tex, USA, 2009.

[2] R. Gee, C. Hanley, R. Hussain, L. Canuel, and J. Martinez, "Axial oscillation tools vs. Lateral vibration tools for friction reductionewhat's the best way to shake the pipe," in *Proceedings of the SPE/IADC Drilling Conference and Exhibition*, Society of Petroleum Engineers, London, UK, 2015.

[3] P. Chen, D. Gao, Z. Wang, and W. Huang, "Study on aggressively working casing string in extended-reach well," *Journal of Petroleum Science and Engineering*, vol. 157, pp. 604–616, 2017.

[4] Y. Liu, P. Chen, X. Wang, and T. Ma, "Modeling friction-reducing performance of an axial oscillation tool using dynamic friction model," *Journal of Natural Gas Science and Engineering*, vol. 33, pp. 397–404, 2016.

[5] X. Wang, P. Chen, T. Ma, and Y. Liu, "Modeling and experimental investigations on the drag reduction performance of an axial oscillation tool," *Journal of Natural Gas Science and Engineering*, vol. 39, pp. 118–132, 2017.

[6] H. T. K. Roberto, S. A. D. Abdullah, G. K. Waleed, and H. E. D. Abdelsattar, "Successful application of new sliding technology for horizontal drilling in Saudi Arabia," *Saudi Aramco Journal of Technology*, pp. 28–33, 2011.

[7] R. Samuel, "Friction factors: what are they for torque, drag, vibration, bottom hole assembly and transient surge/swab analyses?" *Journal of Petroleum Science and Engineering*, vol. 73, no. 3-4, pp. 258–266, 2010.

[8] H. Xu, H. Niu, H. Tang, and X. Zhang, "Application of hydraulic oscillators to the development of Well Xinsha 21-28H in the Xinchang Gas Field, western Sichuan Basin," *Natural Gas Industry*, vol. 33, no. 3, pp. 64–67, 2013.

[9] R. Pohlman and E. Lehfeldt, "Influence of ultrasonic vibration on metallic friction," *Ultrasonics*, vol. 4, no. 4, pp. 178–185, 1966.

[10] K. Grudziński and R. Kostek, "Influence of normal micro-vibrations in contact on sliding motion of solid body," *Journal of Theoretical and Applied Mechanics*, vol. 43, no. 1, pp. 37–49, 2005.

[11] W. F. Roper and T. B. Dellinger, "Reduction of the Frictional Coefficient in a Borehole by the Use of Vibration, 1983".

[12] N. Wicks, J. A. Pabon, F. M. Auzerais et al., "Modeling of axial vibrations to allow intervention in extended reach wells,"

in *Proceedings of the SPE Deepwater Drilling and Completions Conference*, Galveston, Tex, USA, 2012.

[13] N. Wicks, J. A. Pabon, and A. S. Zheng, "Modeling and field trials of the effective tractoring force of axial vibration tools," in *Proceedings of the SPE Deepwater Drilling and Completions Conference*, Galveston, Tex, USA, 2014.

[14] E. R. Barakat, S. Miska, Y. Mengjlao, P.-A. Simionescu, and N. Takach, "The effect of hydraulic vibrations on initiation of buckling and axial force transfer for helically buckled pipes at simulated horizontal wellbore conditions," in *Proceedings of the SPE/IADC Drilling Conference and Exhibition 2007*, pp. 254–261, February 2007.

[15] P. R. Dahl, "Solid friction damping of mechanical vibrations," *AIAA Journal*, vol. 14, no. 12, pp. 1675–1682, 1976.

[16] P. Dupont, B. Armstrong, and V. Hayward, "Elasto-plastic friction model: contact compliance and stiction," in *Proceedings of 2000 American Control Conference (ACC 2000)*, pp. 1072–1077 vol.2, Chicago, IL, USA, June 2000.

[17] P. Dupont, V. Hayward, B. Armstrong, and F. Altpeter, "Single state elastoplastic friction models," *Institute of Electrical and Electronics Engineers Transactions on Automatic Control*, vol. 47, no. 5, pp. 787–792, 2002.

[18] C. Canudas de Wit, H. Olsson, K. J. Astrom, and P. Lischinsky, "A new model for control of systems with friction," *Institute of Electrical and Electronics Engineers Transactions on Automatic Control*, vol. 40, no. 3, pp. 419–425, 1995.

[19] J. Swevers, F. Al-Bender, C. G. Ganseman, and T. Prajogo, "An integrated friction model structure with improved presliding behavior for accurate friction compensation," *Institute of Electrical and Electronics Engineers Transactions on Automatic Control*, vol. 45, no. 4, pp. 675–686, 2000.

[20] F. Al-Bender, V. Lampaert, and J. Swevers, "The generalized Maxwell-slip model: a novel model for friction simulation and compensation," *Institute of Electrical and Electronics Engineers Transactions on Automatic Control*, vol. 50, no. 11, pp. 1883–1887, 2005.

[21] W. Littmann, H. Storck, and J. Wallaschek, "Sliding friction in the presence of ultrasonic oscillations: Superposition of longitudinal oscillations," *Archive of Applied Mechanics*, vol. 71, no. 8, pp. 549–554, 2001.

[22] W. Littmann, H. Storck, J. Wallaschek, and D. J. Inman, "Reduction of friction using piezoelectrically excited ultrasonic vibrations," in *Proceedings of the SPIE's 8th Annual International Symposium on Smart Structures and Materials*, pp. 302–311, Billingham, Washington, DC, USA, 2001.

[23] M. Leus and P. Gutowski, "Analysis of longitudinal tangential contact vibration effect on friction force using coulomb and dahl models," *Journal of Theoretical and Applied Mechanics*, vol. 46, no. 1, pp. 171–184, 2008.

[24] P. Gutowski and M. Leus, "The effect of longitudinal tangential vibrations on friction and driving forces in sliding motion," *Tribology International*, vol. 55, pp. 108–118, 2012.

[25] P. Wang, H. Ni, R. Wang, Z. Li, and Y. Wang, "Experimental investigation of the effect of in-plane vibrations on friction for different materials," *Tribology International*, vol. 99, pp. 237–247, 2016.

[26] V. L. Popov, *Contact Mechanics and Friction: Physical Principles and Applications*, Springer, Berlin, Germany, 2010.

[27] P. Flandrin, G. Rilling, and P. Gonçalvés, "Empirical mode decomposition as a filter bank," *IEEE Signal Processing Letters*, vol. 11, no. 2, pp. 112–114, 2004.

[28] S. Mohanty, K. K. Gupta, K. S. Raju, A. Singh, and S. Snigdha, "Vibro acoustic signal analysis in fault finding of bearing using empirical mode decomposition," in *Proceedings of the 2013 International Conference on Advanced Electronic Systems, ICAES 2013*, pp. 29–33, September 2013.

[29] Y. Liu, P. Chen, T. Ma, and X. Wang, "An evaluation method for friction-reducing performance of hydraulic oscillator," *Journal of Petroleum Science and Engineering*, vol. 157, pp. 107–116, 2017.